



HAL
open science

Localization of self-potential sources in volcano-electric effect with complex continuous wavelet transform and electrical tomography methods for an active volcano

Ginette Saracco, Philippe Labazuy, Frédérique Moreau

► **To cite this version:**

Ginette Saracco, Philippe Labazuy, Frédérique Moreau. Localization of self-potential sources in volcano-electric effect with complex continuous wavelet transform and electrical tomography methods for an active volcano. *Geophysical Research Letters*, 2004, 31 (12), pp.L12610. 10.1029/2004GL019554 . hal-03099158

HAL Id: hal-03099158

<https://hal.science/hal-03099158>

Submitted on 6 Jan 2021

HAL is a multi-disciplinary open access archive for the deposit and dissemination of scientific research documents, whether they are published or not. The documents may come from teaching and research institutions in France or abroad, or from public or private research centers.

L'archive ouverte pluridisciplinaire **HAL**, est destinée au dépôt et à la diffusion de documents scientifiques de niveau recherche, publiés ou non, émanant des établissements d'enseignement et de recherche français ou étrangers, des laboratoires publics ou privés.

Localization of self-potential sources in volcano-electric effect with complex continuous wavelet transform and electrical tomography methods for an active volcano

Ginette Saracco

CNRS-CEREGE, Département de Géophysique, Plateau de l'Arbois, Aix-en-Provence, France

Philippe Labazuy

CNRS Laboratoire Magmas and Volcans, OPGC, Université B. Pascal, Clermont-Ferrand, France

Frédérique Moreau

CNRS-UMR 6618, Géosciences-Rennes, Campus de Beaulieu, Rennes, France

Received 21 January 2004; revised 12 May 2004; accepted 18 May 2004; published 26 June 2004.

[1] This study concerns the fluid flow circulation associated with magmatic intrusion during volcanic eruptions from electrical tomography studies. The objective is to localize and characterize the sources responsible for electrical disturbances during a time evolution survey between 1993 and 1999 of an active volcano, the Piton de la Fournaise. We have applied a dipolar probability tomography and a multi-scale analysis on synthetic and experimental SP data. We show the advantage of the complex continuous wavelet transform which allows to obtain directional information from the phase without a priori information on sources. In both cases, we point out a translation of potential sources through the upper depths during periods preceding a volcanic eruption around specific faults or structural features. The set of parameters obtained (vertical and horizontal localization, multipolar degree and inclination) could be taken into account as criteria to define volcanic precursors. *INDEX*

TERMS: 0903 Exploration Geophysics: Computational methods, potential fields; 3260 Mathematical Geophysics: Inverse theory; 6982 Radio Science: Tomography and imaging; 8419 Volcanology: Eruption monitoring (7280); 8424 Volcanology: Hydrothermal systems (8135). *Citation:* Saracco, G., P. Labazuy, and F. Moreau (2004), Localization of self-potential sources in volcano-electric effect with complex continuous wavelet transform and electrical tomography methods for an active volcano, *Geophys. Res. Lett.*, 31, L12610, doi:10.1029/2004GL019554.

1. Introduction: Geological Framework

[2] The Piton de la Fournaise is the active basaltic shield volcano of the Reunion island in the western Indian ocean. Off-shore surveys [Lénat and Bachelery, 1990] show the presence of more than 500 km³ of landslide deposits, that show a succession of cycles of volcanic construction and landslide during the evolution of the eastern flank of Piton de la Fournaise. Inside the Enclos Fouqué caldera, 13 km long and 6–8 km wide, resides the central cone where most of the volcanic activity occurs. This 400 m-high major active zone is placed along two rift zones (SE and NE),

corresponding to a radial fracture system (Figure 1). A second system of concentric fractures exists around Dolomieu (to the east) and Bory (to the west) summit craters (Figure 2). We call, the structure defined by SP measurements the Dolomieu Hydrothermal Barrier (DHB).

[3] Geophysical investigations led Lénat and Bachelery, to confirm the presence of a lateral extent of a storage zone between 1 to 2.5 km, composed of a multitude of connected magma reservoirs beneath the central cone (Figure 1). A Hypothesis of a well-developed hydrothermal system [Lénat and Bachelery, 1990; Michel and Zlotnicki, 1998] was pointed out by geoelectrical experiments and geothermal modelisations, [Lénat et al., 2000; Fontaine et al., 2002]. The extent of the shallow hydrothermal system seems to be limited to the east by a conspicuous geophysical discontinuity, the so-named Dolomieu Hydrothermal Barrier, DHB, revealed by SP measurements. In addition, the geometry of the hydrothermal system is affected by two main eruptive fracture zones that we call SW and E fractures (see Figure 2).

[4] In this study, we assume that an active volcanic system is principally controlled by two phenomena: the coupling between magmatic intrusion and thermo-hydro-mechanical (THM) disturbances [Natale, 1998; Merlani et al., 2001], and the electromagnetic field induced by the current density. This latter is generated by the circulation of

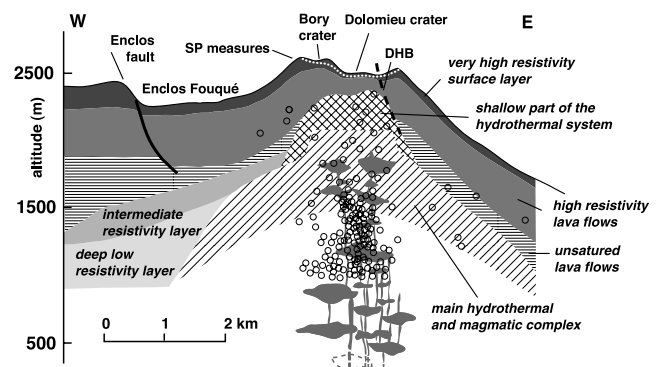


Figure 1. Cross-section of the plumbing system of the Piton de la Fournaise volcano [Lénat et al., 2000].

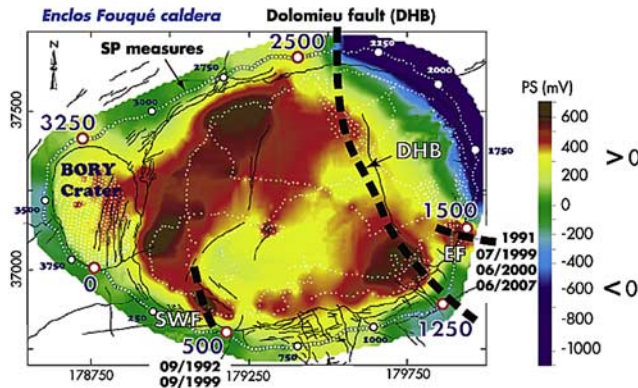


Figure 2. 2D-map of SP data of Dolomieu and Bory craters. Black dashed lines represent the fracture zones, in particular the Dolomieu Hydrothermal Barrier (DHB).

a fluid flow in the porous formation [Mizutani *et al.*, 1976; Michel and Zlotnicki, 1998; Yoshida, 2001; Revil *et al.*, 2003], increased here by the THM process (e.g., variation of the strain or temperature field). 3D studies using a probability tomography concept were performed on the interpretation of natural electromagnetic induction field [Mauriello and Patella, 1999], and on the plumbing system of Mount Vesuvius considering gravity, magnetic and SP survey data [Iuliano *et al.*, 2002].

[5] We are interested here to localize the depth of sources responsible of SP anomalies measured at the ground surface ($z = 0$) of the Piton de la Fournaise volcano, in respect of the fractured and hydrothermal system. Another task is to characterize their degree and inclination, or pattern direction associated to magma intrusion in presence of pressure fronts. Our objective is to obtain from this set of parameters, during time evolution studies of volcanic system, some criteria useful to define electrical precursors. The electrical potential deduced from Maxwell equations under quasi-static limit and generated at the air/earth boundary for an observation point P is given principally by:

$$\phi(\mathbf{r}) = \frac{1}{4\pi} \int_{\Omega} \left(\frac{\mathbf{E}(\mathbf{r}') \cdot \nabla \sigma + \nabla \mathbf{j}_f}{\sigma |\mathbf{r} - \mathbf{r}'|} \right) dV$$

\mathbf{E} is the electrical field ($\mathbf{J} = \sigma \mathbf{E} + \mathbf{j}_f$), \mathbf{j}_f the current density due to the fluid filtration pressure (Darcy law), σ the rock's

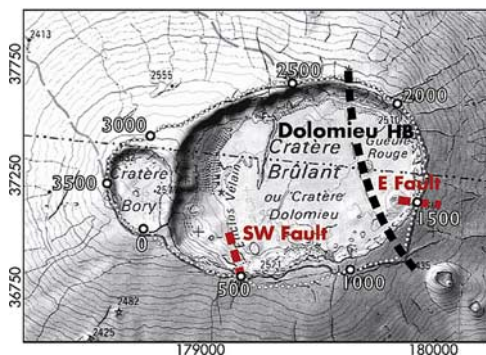


Figure 3. Location of spatial electrography experiments (white dot line). Faults are represented by dashed lines.

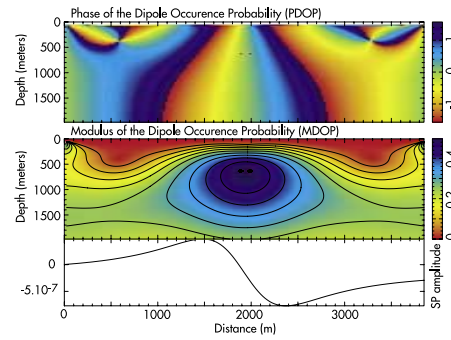


Figure 4. DOP of an horizontal dipole source ($\theta = 90^\circ$), located at the depth $z = 500$ m and $x = 2000$ m.

electrical conductivity and $|\mathbf{r} - \mathbf{r}'|$ the distance between the porous elementary volume V and the observation point P.

2. Electrography Experiments

[6] Several SP surveys were performed between 1993 and 1999, in the most active part of the volcano, during or between eruptive phases. Data were collected with a step of 25 m along a unique closed loop profile of 3.75 km surrounding the two summit Dolomieu and Bory craters (Figure 3). The equipment required was a pair of electrodes (a fixed reference electrode and a portable electrode) connected by wire to a high input impedance voltmeter. Non-polarized porous pot electrodes, made of copper rod immersed in a saturated copper sulphate solution, were used. The potential is measured continually with respect to a fixed point located in a barren area. To obtain the entire profile, five reference bases every 700 m were established. This allows us a minimum of cumulative errors between electrodes.

3. Dipolar Tomography and CCWT

[7] In this section, we recall briefly the principal characteristics of these two tomographic methods applied on a same synthetic example. For more details the reader is referred respectively to Mauriello and Patella [1999], Saracco [1994], Moreau *et al.* [1997], and Sailhac and Marquis [2001].

3.1. Dipolar Tomography Approach (DOP)

[8] Probability tomographic algorithms of self-potential sources were first proposed by Patella in 1997, called charge occurrence probability (COP). The electrical potential ϕ associated to primary and secondary sources can be written: $\phi(r, t) = \sum_{q=1}^N I_q / r_q$, where I_q and r_q describes respectively the intensity of monopole sources and the distance between the source and the observation point.

[9] The associated electrical field is: $\mathbf{E}_u(r, t) = -\nabla_u \Phi(\mathbf{r}, t)$, where u is the local curvilinear coordinate along the profile. The COP function \mathcal{N} is defined as the cross-correlation between this electrical field obtained from potential measures and the theoretical field Γ_u (associated to monopole sources), calculated at each point of the scanned space (x_q, z_q) such that:

$$\mathcal{N}(x_q, z_q) = C_u \int \mathbf{E}_u(x, z(x)) \Gamma_u(x - x_q, z(x) - z_q) dx,$$

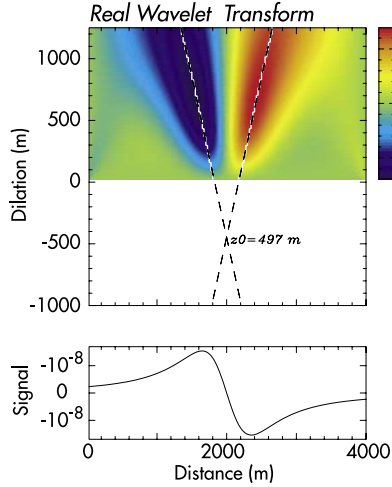


Figure 5. RCWT of the same synthetic source (Figure 4). The intersection of extrema lines allows to localize the source.

where C_u is a coefficient depending on the local site, normalizing the cross-correlation integral, Γ_u the scanner function between the source supposed in $M(x_q, z_q)$ and the potential measure $P(x, z(x))$, $z(x)$ is the topography of the ground.

[10] If the field is due to dipole sources, the electrical potential at a point P in far field approximation is:

$$\Phi_q(\mathbf{r}) = \sum_{q=1}^M \frac{\mathcal{M}_q}{4\pi\epsilon r_q^2} \cos(\theta_q + \beta_q)$$

where \mathcal{M} is the dipolar momentum and ϵ the dielectric constant. θ_q is the angle between the direction defined by PM and the vertical axis, and β_q the angle between the orientation of the dipolar momentum and the vertical axis. In this case we have two scanning functions determined by vertical and horizontal projections. We can define in this context, a Horizontal and Vertical Dipolar Occurrence Probability (DOP), or a Modulus and Phase DOP (Figure 4)

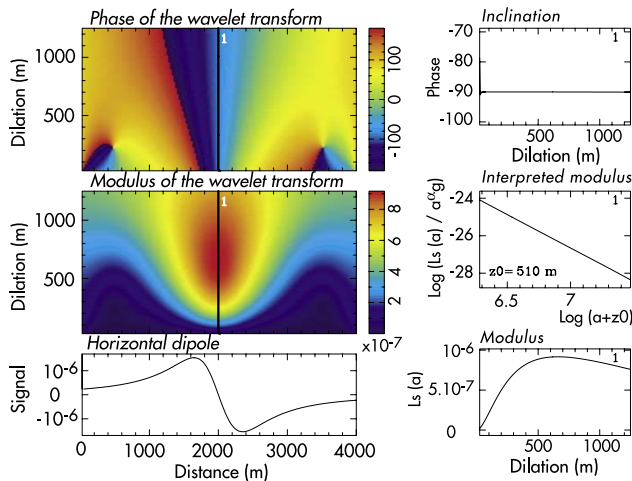


Figure 6. CCWT of the dipole source (Figure 4). From top to bottom *Left*: Inclination $\theta = \text{Phase} + 180^\circ = 90^\circ$, Slope $\alpha = 2$, $L_s(b, a)$ versus dilation.

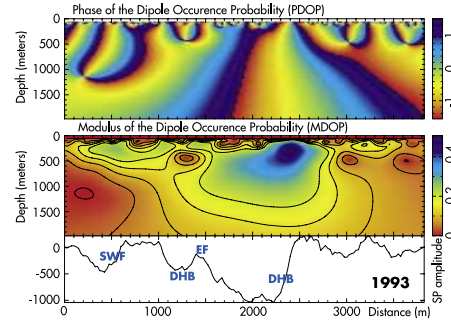


Figure 7. 1993: DOP tomography. Reference level: no eruption. A reservoir (dipolar hydrothermal source) appears centred in $z \simeq 200$ m, $x \simeq 2250$ m with a penetration of 800 m.

comparable respectively to the RCWT (Figure 5) and the CCWT (Figure 6).

3.2. Complex Continuous Wavelet Transform

[11] The continuous wavelet transform L of a signal s , first developed by Grossmann and Morlet in 1983, is: $L_s(b, a) = (D^a g * s)(b)$, where a is the scale parameter associated to the dilation operator D , b the translation parameter and g the real or complex analyzing wavelet.

[12] The properties of covariance of the CWT with respect to both translation and dilation, and the good behavior of wavelet transform of homogeneous function, allows the electrical potential to be defined, using the Poisson equation [Moreau *et al.*, 1997], as:

$$\Phi(x, 0) = \varphi_0(x); \quad \Delta\Phi(x, z) = \sigma(x, z), \quad z < 0,$$

with the homogeneous property $\sigma(\lambda x, \lambda z) = \lambda^\alpha \sigma(x, z)$. It follows:

$$\Phi(x, z) = (D^z P * \varphi_0)(x),$$

where D^z acts on the depth z , with the dilation property: $D^z P * D^z P = D^{z+z} P$. Φ is the harmonic extension of

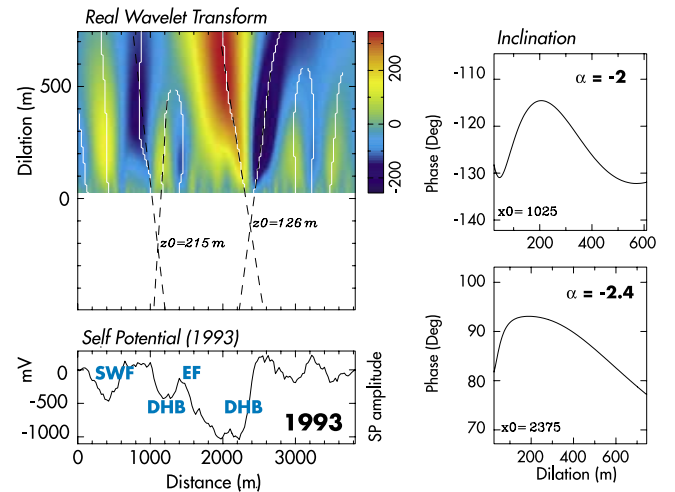


Figure 8. 1993: CCWT of SP data. The DHB ($x \simeq 1050$ m and $x \simeq 2150$ m) is weakly excited. The potential sources are localized around $z \simeq 145$ m. Inclination of sources are *Top*: $\theta = 60^\circ$, *Bottom*: $260^\circ < \theta < 270^\circ$.

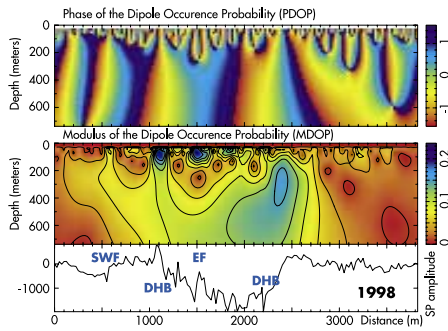


Figure 9. 1998: DOP tomography. Volcanic eruption. SP sources are translated through $z = 0$ along preferential drains.

φ_0 in the half-plane $z > 0$. P is the Poisson Kernel: $P(x) = C_{n+1}(1 + |x|^2)^{-(n+1)/2}$, ($n = 2$ in 3D), with the Fourier transform $P(\mu) = e^{-2\pi|\mu|}$, [Moreau *et al.*, 1997, 1999]. We can see immediately that: x is analogous to a translation parameter T^x , z to a scale parameter D^z . P or derivative of P ($\partial_x^\gamma \partial_z^\beta P$) is the analyzing wavelet “ g ” which is real by construction. Extracting the information from the straight line of extrema of the Real CWT and using the property of harmonic extension in the half plane $z < 0$, allow us to extend those lines in this half-plane and localize the source (Figure 5, dashed lines). Their intersection gives the depth and the horizontal position. The slope in log-log representation gives the multipolar order α of the source (Figure 6, top-left). If we now introduce the Hilbert transform (HT) of this real wavelet, we can define a complex analyzing wavelet: $g_c = \partial_x^\gamma \partial_z^\beta P + iHT(\partial_x^\gamma \partial_z^\beta P)$; $g_c(\mu) = \mu^{\gamma-1} \exp^{-2\pi|\mu|} (i2\pi)^\gamma (\mu + i|\mu|)$, ($\gamma = 2$). A new parameter is obtained from the phase of the CCWT: the inclination θ of potential sources (Figure 6: top-left).

4. Inverse Results

[13] Both tomographic algorithms were applied to experimental data. The CCWT shows the best accuracy in the characterization of sources. However, inverse results are similar in absence of eruption (Figures 7 and 8) with a

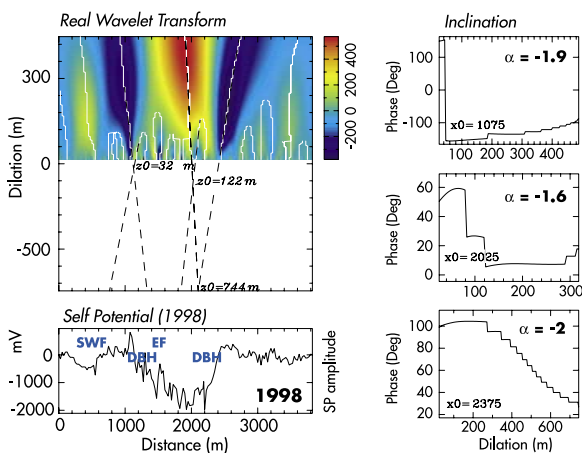


Figure 10. 1998: CCWT of SP data. Volcanic eruption. A phase jump is detected in $x_0 = 1075$ m, $z_0 = 32$ m. Dolomieu and EF are the main drains.

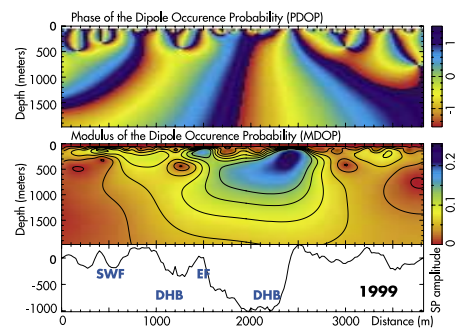


Figure 11. 1999: No eruption. Come back to initial state.

source depth centred at $z \simeq 200$ m and a penetration to $z \simeq 800$ m, corresponding to the DHB ($x \simeq 2150$ m). As the eruptive phase occurred (1998), the sources are translated through the surface $z = 0$ (see Figures 9 and 10) and the E fracture ($x \simeq 1500$ m) and DHB ($x \simeq 1100$ m) are acted like drains with an inclination of $190^\circ < \theta < 240^\circ$ for $x = 2025$ m and $220^\circ < \theta < 280^\circ$ for $x = 2375$ m (Figure 10). Figure 11 is the come back to the initial state as Figure 9.

5. Conclusion and Perspectives

[14] Multi-scale method (CCWT) as DOP have pointed out a translation of sources through upper depths, increasingly dense as the eruption occurs (1998), in accordance to the volcanic plumbing and THM processes (Figures 1 and 2). This translation is accompanied with a phase jump (Figure 10). The CCWT shows the connection between transient SP anomalies and fractured system (SW-EF, DHB) during an eruptive phase. Their maxima are linked with zones of highest surface fracture (DHB). Dolomieu and E fractures play the role of preferential drains. Now in the absence of volcanic eruption (1993, 1999), hydrothermal flux seem concentrated like two small reservoirs located around $z = 200$ m. Could the characterization of translation, inclination and z of SP sources imply an internal dynamic behavior of the Piton de la Fournaise volcano? Could this in turn be criteria allowing the definition of electrical precursors? These primary results give us a new view of the internal dynamic of this volcano.

[15] **Acknowledgments.** We want to thank J. J. Motte, CEREGE for his help on some graphics, the CNRS for its support through national programs ACI *Eaux & Environment* and *CatNat*.

[16] We want to thank particularly A. Grossman for his fruitful discussions on the phase of the wavelet transform.

References

- Fontaine, F., M. Rabinowicz, J. Boulègue, and L. Jouniaux (2002), Constraints on hydrothermal processes on basaltic edifices: Interferences on the conditions leading to hydrovolcanic eruptions at the P.F.V., *Earth Planet. Sci. Lett.*, 200, 1–14.
- Iuliano, T., P. Mauriello, and D. Patella (2002), Looking inside Mount Vesuvius by potential fields integrated probability tomographies, *J. Volcanol. Geotherm. Res.*, 113, 363–378.
- Lénat, J. F., and P. Bachelery (1990), Structure et fonctionnement de la zone centrale du Piton de la Fournaise, *Le Volcan de la Reunion, CRVF, ed. JF Lenat*, 225–296.
- Lénat, J. F., D. Fitterman, D. B. Jackson, and P. Labazuy (2000), Goelectrical structure of the central zone of PFV, *Bull. Volcanol.*, 62, 75–89.
- Mauriello, P., and D. Patella (1999), Principles of probability tomography for natural-source electromagnetic induction fields, *Geophysics*, 64(5), 1403–1417.

- Merlani, A. L., G. Natale, and E. Salusti (2001), Fracturing processes due to temperature and pressure nonlinear waves propagating in fluid-saturated porous rocks, *J. Geophys. Res.*, *106*, 11,067–11,081.
- Michel, S., and J. Zlotnicki (1998), Self-potential and magnetic surveying of La Fournaise volcano (Réunion Island): Correlations with faulting, fluid circulation, and eruption, *J. Geophys. Res.*, *103*, 17,845–17,857.
- Mitzutani, H., T. Ishido, T. Yokokura, and S. Ohnishi (1976), Electrokinetic phenomena associated with earthquakes, *Geophys. Res. Lett.*, *3*(7), 365–368.
- Moreau, F., D. Gibert, M. Holschneider, and G. Saracco (1997), Wavelet analysis of potential fields, *Invest. Probl.*, *13*, 165–178.
- Moreau, F., D. Gibert, M. Holschneider, and G. Saracco (1999), Identification of sources of potential fields with the continuous wavelet transform: Basic theory, *J. Geophys. Res.*, *104*, 5003–5013.
- Natale, G. (1998), The effect of fluid thermal expansivity on thermo-mechanical solitary shock waves in the underground of volcanic domains, *P. Appl. Geophys.*, *152*, 193–211.
- Revil, A., G. Saracco, and P. Labazuy (2003), The volcano-electric effect, *J. Geophys. Res.*, *108*(B5), 2251, doi:10.1029/2002JB001835.
- Sailhac, P., and G. Marquis (2001), Analytic potentials for the forward and inverse modeling of SP anomalies caused by subsurface fluid flow, *Geophys. Res. Lett.*, *28*, 1851–1854.
- Saracco, G. (1994), Propagation of transient waves through a stratified fluid medium: Wavelet analysis of a nonasymptotic decomposition of the propagator, *J. Acoust. Soc. Am.*, *95*(3), 1191–1205.
- Yoshida, S. (2001), Convection current generated prior to rupture in saturated rocks, *J. Geophys. Res.*, *106*, 2103–2120.

P. Labazuy, CNRS Laboratoire Magmas and Volcans, OPGC, Université B. Pascal, F-63038 Clermont-Ferrand, France. (p.labazuy@opgc.univ-bpclermont.fr)

F. Moreau, CNRS-UMR 6618, Géosciences-Rennes, Campus de Beaulieu, Bat 15, F-35042 Rennes, France. (moreau@univ-rennes1.fr)

G. Saracco, CNRS-CEREGE, Département de Géophysique, Plateau de l'Arbois, BP 80, F-13545 Aix-en-Provence, France. (ginet@cerege.fr)